Available online at www.sciencedirect.com
SCIENCE DIRECT
Diamond & Related Materials 15 (2006) 1452 – 1456
DIAMOND AND RELATED MATERIALS
www.elsevier.com/locate/diamond

Microstructure of diamond–SiC nanocomposites determined by X-ray line profile analysis

J. Gubicza [a], T. Ungár [b], Y. Wang [c], G. Voronin [c], C. Pantea [c], T.W. Zerda [c,*]

[a] Department of Solid State Physics, Eötvös University, Budapest, H-1518, Hungary
[b] Department of General Physics, Eötvös University, Budapest, H-1518, Hungary
[c] Department of Physics, TCU, Fort Worth, TX 76129, USA

Received 27 June 2005; received in revised form 24 October 2005; accepted 29 October 2005
Available online 27 December 2005

Abstract

Diamond composites with nanosize diamond crystals and nanosize SiC matrix were obtained at 8 GPa and temperatures varied between 1800 and 2000 °C. Multiple Whole Profile fitting method applied to X-ray diffractograms of sintered composites provided information on crystallite size and population of dislocations. When the temperature was increased at a constant pressure, it led to a growth of crystallite sizes in both phases and reduced population of dislocations. Porosity was limiting hardness of the specimens indicating importance of sample preparation prior to sintering nanosize diamond powders.

Keywords: High pressure high temperature; Diamond crystal; SiC; Superhard materials

1. Introduction

Most commercially available diamond–SiC composites have been synthesized under high pressure, high temperature (HPHT) conditions from micron size diamond and silicon powders. Despite their extraordinary hardness and wear resistance, these composites have relatively low fracture toughness which limits their potential applications. Recently [1], it has been reported that reduction of the average grain size of silicon carbide matrix from 10 μm to 10 nm had little effect on the hardness, Vickers hardness >45 GPa, but significantly increased fracture toughness of the composites from 6 to 12 MPa $m^{1/2}$. SiC matrix is formed as a result of the reaction between silicon and diamond. Submicron crystalline structure of the silicon carbide binding phase has been obtained by: (i) the ball milling of micron size diamond and silicon powders [2]; (ii) liquid silicon infiltration of nano- or micron size diamond powder [3]; (iii) thorough mixing of nanosize diamond and silicon powders followed by HPHT sintering [4]. In this study we will focus on composites produced by the last two methods.

Veprek [5] explained uniquely high fracture toughness and strength of nanocomposites in terms of the Hall–Petch law [6,7]. This law explains increases in fracture toughness and strength through reduction of grain sizes in the composite. It, however, remains obvious that other effects such as the distribution of crystallite sizes and presence of dislocations, their character and concentrations, and porosity need to be considered.

The microstructure of nanocrystalline materials can be effectively studied by X-ray diffraction line profile analysis. Crystallite size and strain effects acting concurrently cause the broadening of a profile. In plastically deformed metals and ceramics the lattice distortions are mainly caused by dislocations, so the strain broadening can be expressed in terms of the parameters of the dislocation structure [8,9]. The anisotropic strain broadening is taken into account by the contrast factors of dislocations [10]. Progress in computing makes it possible to develop procedures for determining the characteristic features of the microstructure by fitting whole diffraction profiles [11–14]. In the present work the Multiple Whole Profile (MWP) fitting method is used in which the measured intensity profiles are fitted by theoretical functions calculated on the basis of the model of microstructure [13,14]. This procedure yields both the crystallite size distribution and the characteristic parameters of the dislocation structure in nanocrystalline materials.

* Corresponding author.
E-mail address: t.zerda@tcu.edu (T.W. Zerda).

0925-9635/$ - see front matter © 2005 Elsevier B.V. All rights reserved.
doi:10.1016/j.diamond.2005.10.064

Previously we have applied the MWP method to analyze structure of diamond and silicon carbide phases of composites produced from micron size diamonds [15]. This methodology is now extended to study structure of both phases in composites obtained from nanosize precursors.

2. Experimental

2.1. Sample preparation and characterization techniques

Diamond–SiC nanocomposites were synthesized from mixtures of nanodiamond powder of sizes less than 100 nm (average grain size 50 nm, MicroDiamant, Switzerland) and nanosize silicon powder (average size 30 nm, Nanostructured Materials, Houston, USA). Diamond nanopowders were obtained by static high-pressure synthesis and are of better quality than conventional nanodiamonds produced by the detonation technique. The concentration of silicon in the initial powder was 10.5 wt.%. Both powders were placed in a drum mixer with tungsten carbide balls of diameter 4 mm. The wet mixing in methanol continued for 100 h. The sole goal of this process was to thoroughly mix the two powders and no attempt was made to reduce the size of diamond and silicon grains. After mixing, methanol was evaporated and the mixture was sintered by HPHT sintering at 1800 and 2000 °C in a high pressure cell.

Diamond–SiC composites were also prepared from micron size diamond and Si powders by the infiltration technique at 1900 °C. Synthetic diamond powders of crystal size 1–2 and 40–60 μm from the Institute for Superhard Materials, Kiev, Ukraine, and silicon powder of particle size less than 44 μm from Alfa Aesar (Ward Hill, MA) were used in this experiment. Silicon powder is placed at the bottom of the high pressure cell and diamond crystals are placed on the top of silicon. When temperature is increased, silicon melts and is pushed upward by external pressure and capillary effect to fill the gaps between diamond crystals. This process is accompanied by a reaction between carbon atoms from the diamond phase and liquid silicon.

Sintering experiments for both nano- and micron size precursors were run in a toroid high pressure cell which consisted of two identical anvils with toroidal grooves and the lithographic stone gasket that matched the contours of the groves [16]. Pressure calibration of the cell was made by recording phase transitions of Bi and PbTe. Temperature calibration was made by measuring temperature in the center of the high pressure cell by a $W_{3\%}Re/W_{25\%}Re$ thermocouple as a function of electric power dissipated in the apparatus. Obtained power–temperature and load–pressure plots were used as the calibration curves for subsequent HPHT sintering.

During the sintering process pressure was raised to the value 8 GPa at room temperature. Next, the samples were heated to the sintering temperature at a rate of 200 °C/s, and the samples were kept at that temperature for 30 s. Finally, temperature was decreased to the room level and the pressure released. The composite materials produced by this method are listed according to the precursors and the infiltration temperature in Table 1.

After sintering samples were grinded to form tablets of diameter 7.5 mm and height 3 mm. Both bases of the tablets were polished using diamond powders and sprays with particle sizes decreasing gradually from 5 to 0.5 μm.

The density of the samples was measured by the Archimedes method on AT261 Delta Range made by Mettler Toledo. The Knoop microindentation hardness was measured on a PMT3 microhardness tester; the load applied to the indenter was 49 N.

High-resolution powder diffraction data were collected on the X3B1 beamline at the National Synchrotron Light Source, Brookhaven National Laboratory. The specimens were mounted on a single-crystal quartz holder. A double Si(111) crystal monochromator was used to obtain a monochromatic beam of 0.69960(1) Å wavelength, as determined from seven well-defined reflections of an Al_2O_3 flat plate standard.

Before reaching the sample, the incident beam was monitored by an ion chamber and the diffracted signal was normalized for the decay of the primary beam. The diffracted beam was reflected by a Ge(111) analyzer crystal before being detected by a NaI scintillation counter. Diffraction data were collected at room temperature in the 2θ range of 13° and 98° with step size of 0.02°.

2.2. Evaluation procedure of X-ray diffraction profiles

The microstructure of the specimens were studied by X-ray diffraction line profile analysis. The *111*, *311*, *331*, *440*, *531*, *620* and *642* peaks of the diamond phase and *111*, *220* and *311* of the silicon carbide phase were evaluated. The small number of peaks of SiC phase used here is due to the fact that the other diffraction peaks of this phase were weak and overlapping with

Table 1
The volume-weighted mean crystallite size ($\langle x \rangle_{vol}$), the dislocation density (ρ) for diamond and SiC phases, the porosity and Knoop hardness (H_K)

Precursors	Sintering	Phase	$\langle x \rangle_{vol}$ [nm]	ρ [10^{14} m^{-2}]	Porosity (%)	H_K [GPa]
50 nm diamond and 30 nm Si powder	Mixture sintering at 1800 °C	Diamond (85 wt.%)	21 (3)	60 (7)	10.5	28 (1)
		SiC (15 wt.%)	12 (1)	40 (5)		
50 nm diamond and 30 nm Si powder	Mixture sintering at 2000 °C	Diamond (85 wt.%)	27 (3)	20 (2)	6.8	28 (1)
		SiC (15 wt.%)	19 (2)	20 (2)		
1–2 μm diamond, 44 μm Si	Infiltration at 1900 °C	Diamond (76%)	41 (4)	33 (5)	2.9	42 (2)
		SiC (24%)	17 (2)	42 (5)		
40–60 μm diamond, 44 μm Si	Infiltration at 1900 °C	Diamond (86%)	106 (10)	9 (1)	0.3	52 (2)
		SiC (14%)	37 (4)	41 (5)		

Uncertainty of the results is indicated by values in the parenthesis.

strong lines of diamond. The evaluation of the peak profiles was performed by the Multiple Whole Profile fitting (MWP) procedure [13,14]. In this method the Fourier coefficients of the measured profiles are fitted by theoretical functions calculated on the basis of a physical model of the microstructure. In this model the crystallites are assumed to have spherical shape with log-normal size distribution and the strains are assumed to be caused by dislocations. Details of the method have been published previously and can be found in Refs. [6] and [7]. As a result of the MWP fitting procedure the median (m) and the variance (σ) of the size distribution, and the density (ρ) of dislocations are obtained. The parameters m and σ are used to calculate the volume weighted mean crystallite size:

$$<x>_{\mathrm{vol}} = m\exp\left(3.5\sigma^2\right). \quad (1)$$

3. Results and discussion

Fig. 1 shows a part of the X-ray diffractograms between 18° and 34° in 2θ for the nanocomposite processed at 1800 °C. The main phase is diamond (solid squares) and the open circles represent the SiC phase formed due to reaction with silicon. The X-ray data indicate a small amount of residual Si (open triangle) in the composite produced. When sintering temperature was increased to 1900 °C and above no residual silicon was detected. Weak peaks of tungsten-carbide (denoted by crosses) appeared in samples that required mixing using WC balls. In specimens prepared by the infiltration technique, which does not require premixing of precursors, in the diffractograms we did not measure WC. The physical model of the MWP fitting procedure may be affected by residual Si and WC inclusions owing to the development of thermal stresses between these inclusions and the grains of diamond or SiC. As the strain fields caused by thermal stresses are short-range, their effect on line broadening is negligible comparing with the influence of dislocations.

The lines of both phases of nanocomposites, diamond and SiC, become narrower with increased processing temperature. This can be observed in Fig. 2a and b where *111* reflections for the diamond and SiC phases, are shown for different initial

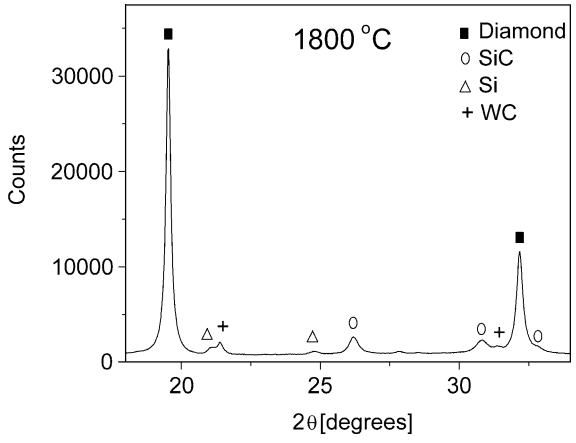

Fig. 1. A part of the X-ray diffractogram corresponding to the 2θ range between 18° and 34° for the nanocomposite sintered at 8 GPa and 1800 °C.

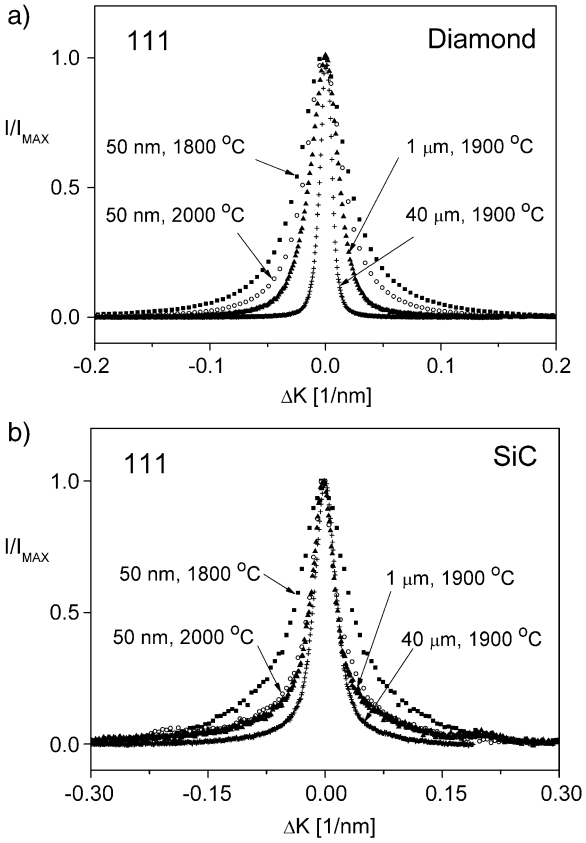

Fig. 2. The *111* line profiles for the diamond (a) and SiC (b) phases produced from precursors with different initial diamond grain sizes and processed at different temperatures (see Table 1). The abscissa is scaled in $\Delta K=(\cos\theta)\,\Delta(2\theta)/\lambda$.

grain sizes and temperatures. For the nanodiamond precursor processed at higher temperatures, the smaller peak widths are resulted by lower strain (dislocation density) rather, than by larger crystallite size. This can be seen from the *modified* Williamson–Hall plot [13] in Fig. 3a where the fitted quadratic curve corresponding to 1800 °C increases steeper than the one corresponding to 2000 °C. For the SiC phase even the low angle reflections are much narrower at higher temperatures due to the significantly larger crystallite size (see Fig. 3b). The *111* reflections corresponding to the diamond phase in the composites produced from micron size powders are also shown in Fig. 2. These profiles are narrower than those measured on composites processed from nanopowders.

The parameters of the microstructure were obtained from the MWP fitting procedure. As an example the fittings for the diamond and SiC phases of the nanocomposite formed at 1800 °C are shown in Fig. 4a and b, respectively. As the diamond–SiC nanocomposites investigated here are texture-free polycrystalline materials, the average contrast factors, C can be used in the evaluation of the dislocation structure [17]. In a texture-free cubic polycrystalline material C can be given as a quadratic function of the hkl indices of reflections. The value of C depends also on the edge or screw character of dislocations in the specimen which is taken into account by a parameter denoted by q. With the values for the elastic stiffness constants given in Refs. [18,19] and assuming that the most common

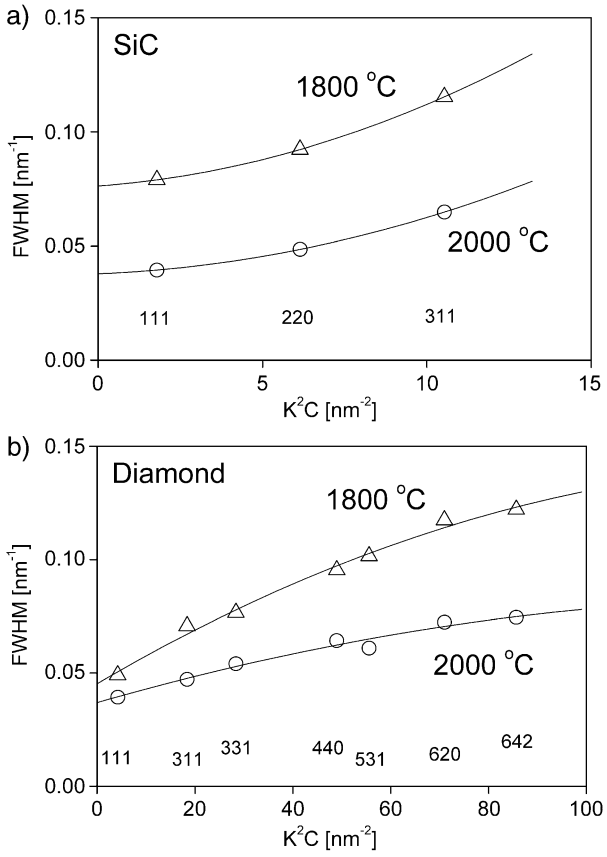

Fig. 3. The *modified* Williamson–Hall plot for diamond (a) and SiC (b) phases of diamond–SiC nanocomposites. $K=2\sin\theta/\lambda$ and C is the average contrast factor [13].

dislocation slip system in both diamond and β-SiC has the Burgers vector $\boldsymbol{b}=a/2<110>\{111\}$ (both diamond and β-SiC have *fcc* unit cells), the values of the q parameter in the contrast factor for pure edge and pure screw dislocations are 0.30 and 1.35 for diamond and 1.1 and 2.1 for β-SiC, respectively [17]. Assuming the half edge-half screw character of dislocations the q values were taken as 0.8 for pure diamond phase and 1.6 for SiC phase. Here we note that if pure edge or screw character of dislocations is assumed for any of the two phases, the quality of the fitting is only slightly changed, and the parameters of the microstructure remain within the error range of ±10% of the values determined for the half edge-half screw case. This is mainly caused by the relatively low elastic anisotropy of diamond and silicon carbide ($A=2c_{44}/(c_{11}-c_{12})=1.2$ and 2.2 for diamond and silicon carbide, respectively). The q values corresponding to the half edge-half screw character of dislocations were also used for the calculation of the C contrast factors in the *modified* Williamson–Hall plots of Fig. 3.

The values of the crystallite size and the dislocation density obtained by the MWP fitting procedure are listed in Table 1. The data show that the sintering carried out at high pressure and high temperature results in diamond–SiC composites with a high dislocation density and nanosize crystallites. The crystallite size of the SiC phase is sensitive to the size of the precursor diamond crystals and is affected by the reaction temperature. The data indicate that with increasing temperature the SiC crystallite size increases and the dislocation density decreases as a result of the dynamic recovery of the nanostructure during the production process. The application of diamond precursor with 40 μm crystallite size results in higher crystallite size of SiC while the dislocation density of this phase is less sensitive to the initial grain size of diamond.

Due to severe plastic deformations caused by HPHT treatment, diamond crystals are divided into a number of crystallites of sizes that primarily depend on applied pressure [20]. All experiments discussed in this study were conducted at 8 GPa and differences in crystallite sizes listed in Table 1 are caused by different temperature and initial average size of the crystals. As in the case of SiC, increased temperature results in larger diamond crystallites and reduced population of dislocations. Fragmentation of micron size diamond crystals ~~o~~ to nanosize crystallites is the result of intense plastic deformation during heating at high pressure [20]. This behavior of diamond at high temperatures and pressures seems to be similar to metallic materials during severe plastic deformation at ambient temperatures [13].

From the density of the specimens we calculated porosity of the samples, which are listed in Table 1. Large values of porosity indicate that at lower temperatures silicon does not fill all the pores between diamond grains, which is also supported

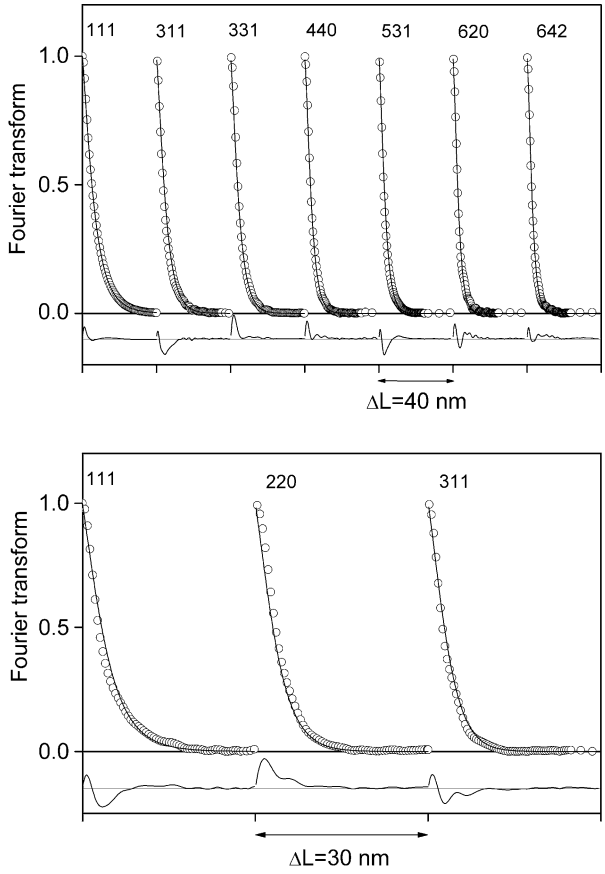

Fig. 4. Measured (open circles) and fitted (solid line) Fourier transforms of the diamond (a) and SiC (b) diffraction profiles for the nanocomposite formed at 1800 °C. The difference between the measured and the fitted curves is shown in the bottom part of the figures.

by the presence of residual silicon indicated by Si peaks in the X-ray diffractograms (see above).

The hardness values for the specimens are also listed in Table 1. It was expected that the hardness would increase with decreasing crystal sizes, but just an opposite effect was observed. When diamond crystals of average diameter of 40 μm were used the hardness of the composite was 52 GPa, but for nanocomposites it was only 28 GPa. The hardness of nanocomposites produced at different temperatures was equal within experimental error, which is the result of the fortuitous compensation of the strengthening caused by lower crystallite size (and the higher dislocation density as well) and the weakening effect caused by the higher porosity of the specimen produced at 1800 °C. We explain the softening of the composites of decreasing grain size as a result of increasing porosity.

Manufacturing of nanosize diamond composites remains a difficult task that requires further improvements. Although addition of nanosize diamonds to the manufacturing protocol may result in improved hardness and fracture toughness [1,5], it may also cause increased porosity that weakens mechanical properties of the composite. Increased porosity is connected to the so-called 'bottle neck' effect. Although the two precursors, diamond and silicon nanosize powders, were thoroughly mixed, a reaction between nanosize diamond and silicon results in SiC which may restrict motion of liquid silicon and thus result in cavities. Increased temperature leads to a reduction of silicon viscosity allowing for a more efficient penetration of the specimen and thus more uniform distribution of SiC. When larger diamond crystals are used then the average diameter of the channels through which liquid silicon can flow are sufficiently large and cannot be easily closed by the SiC phase formed as a result of reactive sintering. It is noted, however, that the lower hardness of the specimen produced from 1 μm diamond powder compared to that obtained from the powder of 40 μm initial size can be attributed to both the higher porosity and higher SiC content.

4. Conclusions

Diamond composites with nanosize diamond crystals and nanosize SiC matrix were obtained at high pressure, high temperature conditions. Extreme manufacturing conditions resulted in reduction of crystallite sizes and induced large population of dislocations in both diamond and silicon carbide phases. When at a constant pressure, the temperature was increased, it led to a growth of crystallite sizes in both phases and reduced population of dislocations.

Composites produced from diamond powders with micron size grains show higher hardness due to smaller porosity [2,4,5]. To avoid composites softening caused by porosity, the two precursors must be thoroughly mixed and silicon must be evenly dispersed prior to the sintering. Increased temperature of the reaction may also reduce porosity through lower viscosity of liquid silicon enabling it reaching even the most restrictive cavities before the reaction product, SiC, could clock them.

Acknowledgements

This study was partially supported by the Hungarian Scientific Research Fund, OTKA, grants F047057, T043247 and T046990, and by NSF grant DMR 0502136. Use of the National Synchrotron Light Source, Brookhaven National Laboratory, was supported by the U.S. Department of Energy, Office of Science, Office of Basic Energy Sciences, under Contract No. DE-AC02-98CH10886. The SUNY X3 beamline at NSLS is supported by the Division of Basic Energy Sciences of the US Department of Energy under Grant No. DE-FG02-86ER45231.

References

[1] Y. Zhao, J. Qian, L. Daemen, C. Pantea, J. Zhang, G. Voronin, T.W. Zerda, Appl. Phys. Lett. 84 (2004) 1356.
[2] J. Qian, G. Voronin, T.W. Zerda, D. He, Y. Zhao, J. Mater. Res. 17 (2002) 2153.
[3] E.A. Ekimov, A.G. Gavriluk, B. Palosz, S. Gierlotka, P. Dluzewski, E. Tatianin, Y. Kluev, A.M. Naletov, A. Presz, Appl. Phys. Lett. 77 (2000) 954.
[4] G.A. Voronin, T.W. Zerda, J. Qian, Y. Zhao, D. He, S.N. Dub, Diamond Relat. Mater. 12 (2003) 1477.
[5] S. Veprek, in: R. Riedel (Ed.), Handbook of Ceramic Hard Materials, Chap. 4, Wiley-VCH, Weiheim, 2000.
[6] E.O. Hall, Proc. Phys. Soc., Lond. 64B (1951) 747.
[7] N.J. Petch, Iron Steel Inst., Lond., Bibliogr. Ser. 174 (1953) 25.
[8] M.A. Krivoglaz, Theory of X-ray and Thermal Neutron Scattering by Real Crystals, Plenum Press, New York, 1996.
[9] M. Wilkens, Phys. Status Solidi, A Appl. Res. 2 (1970) 359.
[10] R. Kuzel Jr., P. Klimanek, J. Appl. Crystallogr. 21 (1988) 363.
[11] J.I. Langford, D. Louër, P. Scardi, J. Appl. Crystallogr. 33 (2000) 964.
[12] P. Scardi, M. Leoni, Acta Crystallogr., A 58 (2002) 190.
[13] T. Ungár, J. Gubicza, G. Ribárik, A. Borbély, J. Appl. Crystallogr. 34 (2001) 298.
[14] G. Ribárik, T. Ungár, J. Gubicza, J. Appl. Crystallogr. 34 (2001) 669.
[15] G.A. Voronin, T.W. Zerda, J. Gubicza, T. Ungar, S.N. Dub, J. Mater. Res. 19 (2004) 2703.
[16] L.G. Khvostantsev, High Temp. High Press. 16 (1984) 165.
[17] T. Ungár, I. Dragomir, Á. Révész, A. Borbély, J. Appl. Crystallogr. 32 (1999) 992.
[18] H.J. McSkimin, W.L. Bond, Phys. Rev. 105 (1957) 116.
[19] D.H. Chung, W.R. Buessem, Anisotropy of Single Crystal Refractory Compounds, Plenum Press, New York, 1968, p. 2.
[20] C. Pantea, J. Gubicza, T. Ungár, G. Voronin, T.W. Zerda, Phys. Rev., B 66 (9) (2002) (art. no. 094106).